Spectrochimica Acta Part A: Molecular and Biomolecular Spectroscopy 110 (2013) 430–436

Contents lists available at SciVerse ScienceDirect

Spectrochimica Acta Part A: Molecular and Biomolecular Spectroscopy

journal homepage: www.elsevier.com/locate/saa

Synthesis, spectroscopic characterization and DFT calculations of β-O-4 type lignin model compounds

Fatemeh Mostaghni, Abbas Teimouri *, Seyed Ahmad Mirshokraei

Chemistry Department, Payame Noor University, 19395-4697 Tehran, Islamic Republic of Iran

HIGHLIGHTS

- We propose the new and easy reaction for synthesis of β-O-4 lignin model compounds.
- Two model compounds is synthesised and characterize by IR, Mass and NMR spectroscopy.
- Density functional theory (DFT) calculations have been carried out.
- The results indicates DFT gives satisfactory results for these compounds.
- These data will improve methods of synthesis and understanding of paper industry.

GRAPHICAL ABSTRACT

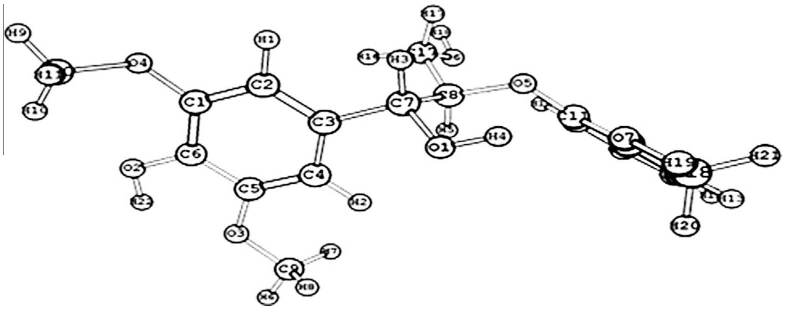

ARTICLE INFO

Article history:
Received 10 November 2012
Received in revised form 9 February 2013
Accepted 17 March 2013
Available online 25 March 2013

Keywords:
Lignin model compounds
β-O-4 structure
Lignin synthesis
β-O-4 linkage
Arylglycerol-β-guaiacyl ether
DFT

ABSTRACT

β-O-4 type lignin model compounds with the title of Erythro-2-(2-methoxyphenoxy)-1-(3,4,5-trimethoxyphenyl)-1,3-propanediol and Erythro-2-(2-methoxyphenoxy)-1-(4-Hydroxy-3,5-dimethoxyphenyl)-1,3-propanediol were synthesised and some modifications and improvements on them were introduced. These compounds were characterized by IR, Mass and NMR spectroscopy. Density functional theory (DFT) calculations were performed for the title compounds using the standard 6-31G* basis set. IR, ^{13}C and ^{1}H NMR of the title compounds were calculated at the DFT-B3LYP level of theory using the 6-31G* basis set. In this work comparison between the experimental and the theoretical results indicates that the DFT-B3LYP method is able to provide satisfactory results for predicting the properties of the considered compounds.

Introduction

Lignin is one of the main cell wall components in woody plants. It is considered to be the second most abundant biopolymer after cellulose. Lignin has a very complex three dimensional structure consisting of three aromatic groups, i.e. p-coumaryl alcohol, coniferyl alcohol and sinapyl alcohol depending on the wood type. These precursors are called monolignols and contribute to guaiacyl, syringyl and p-hydroxyphenyl propane units in lignin, respectively. Softwood lignin is produced mainly from coniferyl alcohol and hardwood lignin is made mainly from coniferyl alcohol and sinapyl alcohol. In addition to these two monolignols, p-coumaryl alcohol contributes to lignin in herbaceous plants. These monolignols are considered to be polymerized via a random dehydrogenative reaction mechanism to produce the complicated biomacromolecule lignin which is distributed nonuniformly as the result of anatomical structure. The main interunit linkages are called β-O-4, β–β, β-5, β-1, 5–5, 4-O-5 linkages and so on. Beyond the structural function, lignin plays several other important

---

* Corresponding author. Tel.: +98 311 3521804-6; fax: +98 311 3521802.
E-mail address: a_teimouri@pnu.ac.ir (A. Teimouri).

1386-1425/$ - see front matter © 2013 Elsevier B.V. All rights reserved.
http://dx.doi.org/10.1016/j.saa.2013.03.075

biological roles in plants. Because it is much less hydrophilic than cellulose and hemicellulose, it prevents the absorption of water by these polysaccharides in plant cell walls and allows the efficient transport of water in the vascular tissues. Lignin also forms an effective barrier against attack by insects and fungi. Although lignin is necessary to trees, it is undesirable in most chemical papermaking fibers and is removed by pulping and bleaching processes [1].

The heterogeneity of lignin is caused by variations in the polymer composition, size, cross linking and functional groups. Thus our knowledge of lignin chemical structure is less precise than our knowledge of other natural and synthetic polymers.

The high sensitivity of mechanical pulps and clear woods towards sunlight exposure is a well described process. It is generally accepted that the photo yellowing of lignocellulosics is mainly due to the photo oxidation of lignin [2–4]. This behavior is associated to the presence of lignin functional groups that interact with the UV portion of sunlight in the region between 300 and 400 nm. Due to the industrial and environmental relevance of to the formation of processes involving lignin degradation and discoloration such as pulping, bleaching and photoyellowing, a considerable effort has been made towards the understanding of their mechanistic aspects, photo- and radiation chemical methods being particularly useful for the study of these processes. However, because of the complexity of the lignin, the detailed studies of the reactions involved in these processes are difficult.

The structure and chemistry of lignin have been described in terms of results from a wide range of chemical or spectroscopic methods to construct a mosaic picture of the polymer. There are many studies available in the literature involving degradation of lignins to low molecular weight compounds in order to obtain structural information. Lignin dimers and trimers which contained most of the major inter-unit linkages have been extensively reported from hydrogenolysis [5] and other methods [6–12] that can be quite expensive and time-consuming. However, knowledge about minor lignin inter-unit linkages is still incomplete.

The determination of the structural built-up of lignin had been a constant challenge for more than a hundred years. One of the main difficulties is the lack of the adequate lignin isolation methods without having the lignin undergoing secondary reactions. The knowledge of lignin structural motifs makes possible the study of its reactivity by using suitable lignin model compounds (LMCs), relatively simple molecules containing isolated functional groups and/or typical lignin bonding patterns.

The use of adequate lignin model compounds is often crucial in lignin research. Lignin model compounds are not commercially available and therefore have to be prepared in the laboratory. In general only small amounts of model compounds are required [13]. Thus the obvious criteria for choosing suitable synthetic routes for such compounds would seem to be simplicity of preparation and ease of purification rather than high yield.

The arylglycerol-β-aryl ether type of lignin has been considered to constitute the most prominent substructure in lignin for a long time [14]. Lignin model compounds of arylglycerol-β-aryl ethers are therefore useful in research concerning lignin. Syntheses of such compounds have been described by several authors [15–20].

Studies of lignin structure and reactivity have been re-energized by the emergence of modern technologies, new analytical methods, and by exciting recent findings. Theoretical methods represent another tool that can be used to complement other techniques, a strategy that has found extensive applications in other branches of chemistry.

Although there may be a tendency to consider experiment and theory as two distinct approaches with little in common, the boundary is becoming increasingly blurred as calculations are extensively integrated with experiment.

In this study the title compounds were synthesised and characterized by IR, Mass and NMR spectroscopy. Density functional theory (DFT) calculations were performed for the title compounds using the standard 6-31G* basis set. IR, ^{13}C and ^{1}H NMR of the title compounds were calculated at the DFT-B3LYP level of theory using the 6-31G* basis set.

Experimental

Materials

All chemicals and solvents were purchased from Aldrich and Merck. Tetrahydrofuran was freshly distilled over sodium. Silica gel for flash chromatography was Merck Kieselgel 60 (230–400 mesh). Thin layer chromatography (TLC) was performed on silica gel plates (Merck, Kieselgel 60 GF254) with dichloromethane/ethyl acetate (9/1) as eluent. Spots were made visible with UV light.

Melting points were determined on electro thermal apparatus. The spectral measurements were performed with a FT Infrared Spectroscope, JASCO, FT/IR-6300 (400–4000 cm^{-1}), Japan. All NMR spectra were recorded on Bruker DRX 500 AVANCE spectrometer. deuterated dimethyl-sulphoxide and chloroform was used as solvent and tetraethyl silane as internal reference. Mass spectra were measured using an AEI MS 902 instrument and this equipment was also used for accurate mass measurements of molecular ions.

Methods

(2-Methoxyphenoxy) acetic acid (1)

(2-Methoxyphenoxy) acetic acid was prepared from guaiacol and chloroacetic acid according to a procedure described [16]. Recrystallization of the residue from water gave product melting at 123–124 °C (yield: 83%).

IR (KBr): 3060 (w), 3011 (w), 2913 (w), 1743 (vs), 1590 (w), 1510 (vs), 1457 (m), 1426 (s), 1250 (vs), 1230 (vs), 1130 (s), 1025 (m), 754(s). ^{1}HNMR ($CDCl_3$): δ 3.92 (3H, s, OCH_3), 4.74 (2H, s, CH_2), 6.95 (1H, m), 6.97 (1H, s), 7.06 (1H, m), 7.29 (1H, s), 10.5 (1H, s, COOH)

Z-2-(2-methoxyphenoxy)-3-(3,4,5-trimethoxyphenyl)-2-propenoic acid (2)

A 250 ml three-necked flask was used in the experiments. The flask was equipped with an inlet and an outlet for nitrogen, a septum for injection of reagents. A slow stream of nitrogen was allowed to pass through the reaction vessel (the flow rate was registered by means of a silicone oil seal). Using a syringe, n-Butyl lithium in THF (42 mmol, 24 ml 1.6 M solution) was injected in to the solution of hexamethyldisilazane (8.28 ml, 40 mmol) in THF (50 ml). To achieve α-lithiation of the carboxylic acid, the mixture was stirred magnetically for about 0.5 h. A solution of (2-methoxyphenoxy) acetic acid (3.65 g, 20 mmol) in THF (25 ml) was slowly injected into the flask. The mixture was kept at −75 °C for 0.5 h (magnetic stirring). The stirring was continued for 1.5–2 h at 45–50 °C and after cooling to −75 °C, a solution of the methylated syringaldehyde (20 mmol, 3.92 g) in THF (15 ml) was slowly added to the reaction mixture. Stirring was continued for 1 h at −75 °C, after which the mixture was stirred at room temperature overnight, it was cooled to 0 °C and acidified to pH = 2 with 3 M HCl. The organic layer was separated and the aqueous layer was extracted with diethyl ether (100 + 3 × 50 ml). The combined organic layers were extracted with 0.2 M NaOH (3 × 75 ml). The extract was acidified with 3 M hydrochloric acid (21 ml) and extracted with ether (250 ml + 3 × 100 ml). The extract was dried (Na_2SO_4)

and solvents were removed by film evaporation that gave an oily residual. The crude product was chromatographed on a silica gel, eluents dichloromethane/ethyl acetate (9:1) and (5:1)] which gave an essentially pure Z isomer (yield, 50%).

^{1}HNMR ($CDCl_3$): δ 3.929 (3H, s, OCH_3), 3.948 (3H, s, OCH_3), 3.961 (3H, s, OCH_3), 3.969 (3H, OCH_3), 6.93–7.39 (7H, m, vinyl, H–Ar), 9.89 (1H, s, COOH). ^{13}CNMR($CDCl_3$): δ 56.66 (OCH_3), 56.69 (OCH_3), 61.35 (OCH_3), 67.75 (OCH_3), 107–154 (Ar), 171.75 (C=C), 173.50 (C=C), 191.70 (COOH).

Erythro-2-(2-methoxyphenoxy)-1-(3, 4, 5-trimethoxyphenyl)-1, 3-propanediol (3a)

Acid 1 (1.2 mmol, 0.5 g) was dissolved in THF (13 ml) in a 100 ml flask and 2 M borane-dimethyl sulfide complex in THF (5 ml) was injected into the flask with a syringe during 15 min (nitrogen atmosphere and magnetic stirring). The reaction mixture was kept at 35 °C for 2 h. Excess of reagents was decomposed by the addition of (1 ml) H_2O. Then H_2O_2 (1 ml 30% H_2O_2) and NaOH 3 M (3 ml) was added over a 30 min period. The reaction mixture was stirred vigorously at 35 °C for 3 h period and transferred to a separatory funnel with 30 ml H_2O and 30 ml $CHCl_3$. The layers were separated and the aqueous layer extracted with 2 × 50 ml $CHCl_3$. The organic layers were combined and dried over Na_2SO_4 and the solvent was removed by film evaporation. The product crystallized on standing. Recrystallization from ethyl acetate yielded crystals yellow needles (yield, 75%).

IR (KBr): 3445 (b), 2931 (m), 2850 (w), 1574 (s), 1516 (s), 1467 (s), 1426 (s), 1364 (s), 1333 (vs), 1267 (m), 1204 (vs), 1119 (vs), 1035 (w). ^{1}HNMR ($CDCl_3$): δ 2.04 (3H, s, CH_3CO), 2.09, (3H, s, CH_3-CO), 3.89 (3H, s, OCH_3), 3.93 (6H, s, OCH_3), 3.94 (3H, s, OCH_3), 4.25 (1H, dd, J = 3.6 and 11.9 Hz, Hγ), 4.39 (1H, dd, J = 5.8 and 11.9 Hz, Hγ), 4.58 (1H, m, Hβ), 6.05 (1H, d, J = 4.8, Hα), 6.84 (2H, s, H–Ar) 6.87–6.99 (4H, m, Ar–H). Mass ($CDCl_3$): m/e (%); $(M)^+$ 364 (0.4), 344(9), 239 (14.6), 195 (100), 167 (5.3), 124 (10.8), 109 (15.46).

Tetrahydropyran-2-yl ether of syringaldehyde

Syringaldehyde was derivativsed essentially according to a method for the preparation of tetra hydro pyran-2-yl ethers of alcohols [21]. (yield, 75%).

^{1}HNMR($CDCl_3$): δ 1.64 (2H, m), 1.84 (2H, m), 2.02 (2H, m), 3.95 (3H, s,OCH_3), 3.98 (3H, s, OCH_3), 4.24 (2H, m), 5.64(1H, d, J = 7.5), 7.15 (2H, s, Ar–H) 9.83 (1H, s).

Erythro-1-(4-Hydroxy-3,5-dimethoxyphenyl)-2-(2-methoxyphenoxy)-1,3-propanediol (3b)

The above procedure for the synthesis of arylglycerol-β-guaiacyl ethers was followed using tetrahydropyran-2-yl ether of syringaldehyde as the primary material, but instead of 3 M HCl, the equivalent amounts of 2 M H_2SO_4 were used for acidification and the reaction mixture was exposed to acid conditions for about 1 h during the workup procedure. Purification of crude product by flash chromatography using mixtures of methylene chloride and ethyl acetate as eluents gave essentially pure **2b** (yield, 37%).

Reduction of acid 2b with boran-dimethylsulfide complex gave an essentially pure product 3b (yield 72%).

IR (KBr): 3424 (s), 2932 (m), 2850 (w), 1575 (s), 1518 (s), 1467 (s), 1426 (s), 1366 (s), 1333 (vs), 1267 (m), 1204 (vs), 1119 (vs), 1034 (w). ^{1}HNMR (DMSO): δ 3.624 (2H, m, Hγ), 3.76 (3H, s, OCH_3), 3.80 (6H, s, OCH_3), 4.276 (1H, m, Hβ),4.57 (1H, t, J = 5.6 Hz, OHγ), 4. 72 (1H, t, J = 4.8 Hz, Hα), 5.26 (1H, d, J = 4.8 Hz, OHα), 6.53 (2H, s, H–Ar), 6.81-6.90 (4H, m, H–Ar), 8.306 (Ar–OH). ^{13}CNMR (DMSO): δ 55.77 (OCH3), 56.26 (OCH_3), 56.26 (OCH_3), 61.22 (Cγ), 65.58 (Cα), 71.33 (Cβ), 103.80 (A2), 103.80 (A6), 111.77(B2), 114.70 (B5), 121.10 (B6), 121.96 (B1), 132.09 (A1), 134.11 (A4), 147.10 (A3), 147.10 (A5), 148.01 (B4), 149.69 (B3).

Quantum mechanical calculations

All calculations were carried out using the Gaussian 09 quantum chemistry package and Gaussian Viewer as graphical medium. DFT calculations were performed by using the three parameter Becke 3LYP functional, which is a hybrid of exact (Hartree-Fock) exchange terms and gradient-corrected exchange and correlation terms, similar to that first suggested by Becke. The usual 6-31G* basis set was employed in the DFT calculations. Following the standard nomenclature the latter calculation will be referred to as B3LYP/6-31G*.

Finally, the calculated normal mode vibrational frequencies, NMR and thermodynamic properties were also calculated with the same method of calculations. Calculated results extracted manually and by using Chemcraft software version 1.6. The computed results have been compared with the experimental data.

Results and discussion

Procedure of easy and stereo selective synthesize of lignin model compounds **3a** and **3b** is shown in two steps on Scheme 1.

The products obtained according to previous studies was a mixture of the two possible diastereomers erythro and threo forms. Pure erythro and threo forms of arylglcerol β-aryl ethers could be isolated forms of reduction products by chromatography on SiO_2 followed by ion-exchange chromatography [15–20].

In this work the intermediate unsaturated acids 2a and 2b were obtained in a pure crystalline state. We used hexamethyldisilazane with no α-proton, as base in condensation step. This preclude of secondary reactions and increase the yield of the condensation step and a diastereoisomeric control can occur using a more sterically crowded enolate that create Z-isomer of propionic acids (**2a, 2b**). The product obtained on hydroboration of compound 2 was identified as the erythro form of compounds. Since hydroboration is known to proceed by syn addition.

The phenolic model Erythro-1-(4-Hydroxy-3,5-dimethoxyphenyl)-2-(2-methoxyphenoxy)-1,3-propanediol (**3b**) was synthesised using the tetrahydropyran-2-yl ether of syringaldehyde and (2-methoxyphenoxy) acetic acid. No separate deprotection step was required since removal of the tetrahydropyran-2-yl group occurred spontaneously during the reaction of tetrahydropyran-2-yl ether of syringaldehyde with α-lithiated 1 (or during the work-up

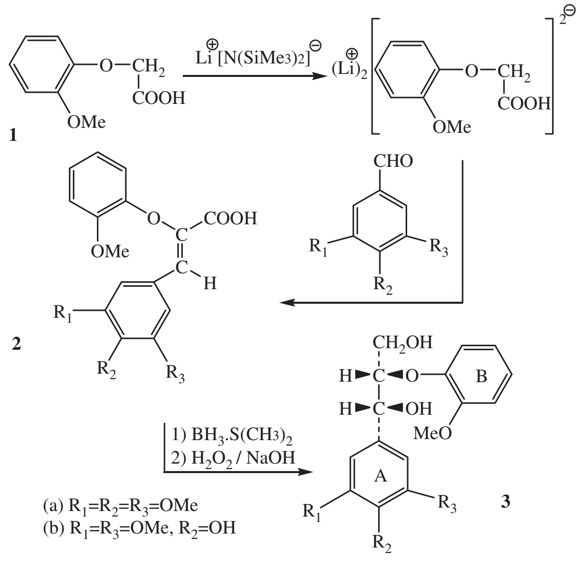

Scheme 1. Stereo selective synthesize of lignin model compounds **3a** and **3b**.

Table 1
Selected bond distances.

Bond lengths	**3a**	**3b**	Bond lengths	**3a**	**3b**
C_1-C_2	1.402	1.402	C_9-C_{10}	1.553	1.552
C_2-C_3	1.393	1.394	$C_{10}-C_{34}$	1.522	1.522
C_3-C_4	1.405	1.407	$C_{34}-O_{37}$	1.429	1.429
C_4-C_5	1.396	1.391	$C_{10}-O_{23}$	1.435	1.435
C_5-C_6	1.413	1.406	$O_{23}-C_{24}$	1.374	1.374
C_6-C_1	1.399	1.397	$C_{24}-C_{25}$	1.414	1.414
C_5-O_{13}	1.365	1.375	$C_{24}-C_{26}$	1.394	1.394
C_6-O_{12}	1.373	1.367	$C_{25}-O_{39}$	1.364	1.364
$O_{13}-C_{14}$	1.423	1.424	$O_{39}-C_{40}$	1.420	1.420
C_1-O_{18}	1.374	1.373	$C_{25}-C_{27}$	1.399	1.399
$O_{12}-C_{47}$	1.435	–	$C_{27}-C_{30}$	1.400	1.400
C_9-O_{44}	1.422	1.423	$C_{30}-C_{28}$	1.393	1.393
C_3-C_9	1.529	1.530	$C_{28}-C_{26}$	1.400	1.400

Table 2
Selected bond angles and Torsional angles.

Bond lengths	**3a**	**3b**	Bond lengths	**3a**	**3b**
$C_9-C_{10}-O_{23}$	108.8	108.9	$C_{25}-C_{27}-C_{30}$	120.3	120.3
$C_3-C_9-O_{44}$	113.4	113.1	$C_{24}-C_{26}-C_{28}$	120.4	120.4
$C_{10}-C_9-O_{44}$	112.1	111.8	$C_{30}-C_{28}-C_{26}$	119.6	119.6
$C_{10}-C_{34}-O_{37}$	108.1	108.0	$C_4-C_3-C_9$	119.0	119.7
$C_{34}-C_{10}-O_{23}$	108.8	108.8	$C_4-C_5-C_6$	120.1	121.1
$C_9-C_{10}-C_{34}$	113.3	113.3	$C_2-C_3-C_9$	121.8	121.4
$C_3-C_9-C_{10}$	112.0	112.4	$C_3-C_4-C_5$	120.6	119.9
$C_6-C_1-O_{18}$	121.2	122.1	$C_{25}-C_{24}-C_{26}$	119.9	119.9
$C_5-O_{13}-C_{14}$	118.5	118.6	$C_6-C_1-C_2$	120.6	119.7
$C_{10}-O_{23}-C_{24}$	118.2	118.2	$C_{27}-C_{30}-C_{28}$	120.3	120.3
Dihedral angles					
$C_3-C_9-C_{13}-C_{15}$	77.19	76.06	$O_{11}-C_9-C_{13}-C_{15}$	−162.81	−52.49
$C_3-C_9-C_{13}-O_{20}$	1161.50	−162.6	$O_{18}-C_{15}-C_{13}-C_9$	−51.68	−162.91
$C_{21}-O_{20}-C_{13}-C_9$	112.2	111.56	$O_{11}-C_9-C_{13}-O_{20}$	69.60	68.79

procedure). These compounds were characterized by IR, Mass and NMR spectroscopy.

*Molecular structure of **3a** and **3b** compounds*

Here DFT is validated for preliminary studies of structure and reactivity of β-O-4 lignin model compounds. The results is shown that molecular calculation holds great potential for studying lignin and can provide valuable information. The optimized geometry and structural parameters of two compounds calculated by B3LYP/6-31G* level of theory. The selected bond distances (Å) and bond angles (°) are listed in Tables 1 and 2 and the optimized configurations are shown in Fig. 1.

It can be observed that the values of bond angles and other geometrical parameters (bond lengths and dihedral angles) complement the experimental findings and reported results. Selected torsion angles in this compound listed in Table 2. The aromatic rings are well separated and the bond distance for C3–C24 bond is 4.534 Å and 4.588 Å in 3a and 3b, respectively.

Table 3
Comparison of the observed and calculated vibrational spectra for important signals of compounds **3a** and **3b**.

Compound	**3a**		**3b**	
Assignment	DFT	Exp.	DFT	Exp.
υ OHγ	3718	3445	3717	3424
υ OHph	–	3445	3642	3424
υ OHα	3685	3445	3679	3424
υ $C-H_{Ar}$	3075	2931	3075	2932
υ C–H(OMeB)	2970	2850	3043	2850
υ C–H(OMeA)	2924	2850	2990	2850
υ Ring def B	1576	1516	1576	1575
υ Ring def A	1566	1574	1490	1518
Asymmetric CH bending	1481	1467	1462	1467
Aromatic ring vibration B	1422	1426	1422	1426
δ O–Hα, Hα	1366	1364	1368	1366
δ O–Hph	–	–	1361	1366
δ Hα, Hβ(in plan)	1347	1333	1346	1333
δ Hα, Hβ(out of plan)	1293	1333	1296	–
Ring breathing A	1276	1267	1288	1267
υ $C_{Ar}-O$	1205	1204	1206	1204
Ar in plan CH bending A	1121	1119	1120	1119
Ar in plan CH bending B	1040	1035	1118	1031

Assignments of vibrational frequencies

Since FT-IR identifies specific chemical functional groups in polymeric compounds, it has been able to give us an estimate of the most molecular components of a plant. For example, identification of specific bonding patterns and their representative IR spectral signals have been shown for cellulose [21,22], lignin and its precursors [23–26]. The observed experimental and calculated vibrational wave numbers of the optimized geometry and the proposed assignments of the two compounds 1 and 2 are given in Table 3.

The observed and calculated spectra are relevant to each other. Based on the comparison between the calculated and experimental results, assignments of fundamental modes were carried out. The assignment of the experimental frequencies is based on the observed band frequencies in the infrared spectra of this species confirmed by establishing one to one correlation between observed and theoretically calculated frequencies. A linearity between the experimental and calculated wave numbers (i.e., for the whole spectral range considered) can be estimated by plotting the calculated versus experimental wave numbers (Fig. 2). The values of the correlation coefficients indicate good linearity between the calculated and experimental wave numbers (correlation coefficients of 0. 998).

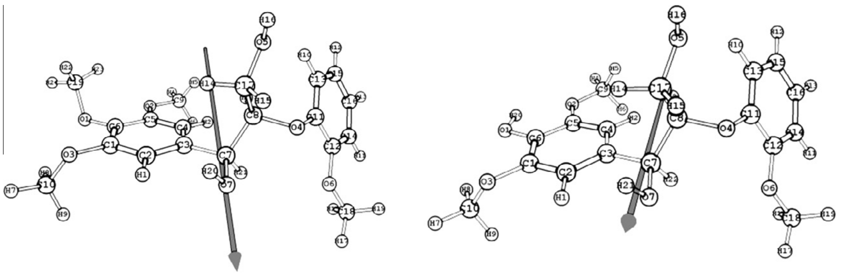

3a

3b

Fig. 1. The structure and dipole moment direction of compounds **3a** and **3b**, optimization has been performed by the B3LYP/6-31G* method.

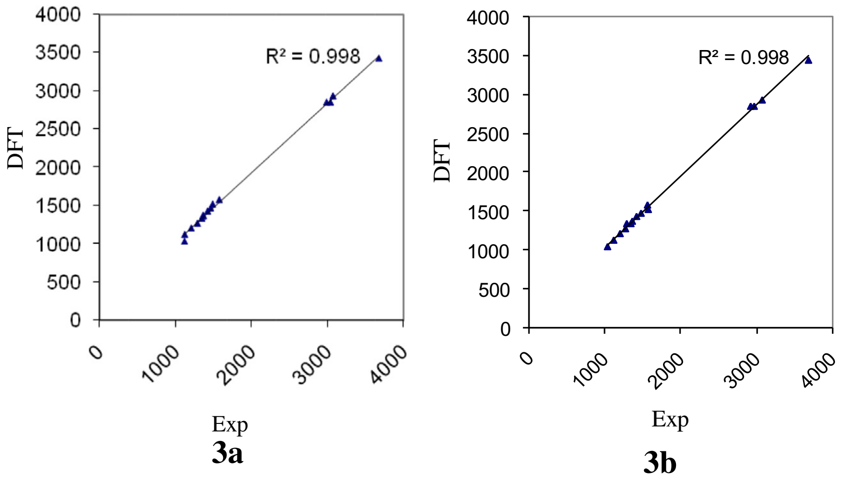

3a **3b**

Fig. 2. Graphic correlation between the experimental and the theoretical frequencies of **3a, 3b** obtained by B3LYP/6-31G* method.

Table 4
Experimental and calculated ^{1}HNMR chemical shifts (ppm) of **3a**, **3b** compounds.

Compound	**3a**		**3b**	
Proton	DFT	Exp.	DFT	Exp.
OH_{Ph}	–	–	5.5	8.3
H_{Ring2}	6.8–8.1	6.8–6.9	6.8–8.2	6.8–6.9
H_{Ring1}	6.6	6.8	6.6	6.5
Hα	5.5	6.0	5.3	4.7
α OH	0.5	–	0.3	5.3
γ OH	0.7	–	0.7	4.6
Hγ	4.1	4.3	4.1	3.6
Hγ	3.8	4.2	3.8	3.6
Hβ	4.3	4.5	4.3	4.2
B OMe	3.9	3.8	3.9	3.7
A OMe	3.8	3.9	3.8	3.8
A OMe	4.0	3.9	4.1	3.8
A OMe	4.1	3.9	–	–

NMR spectra

Experimental and theoretical values for $_1$H, ^{13}C NMR of two compounds **3a** and **3b** are given in Tables 4 and 5.

The theoretical ^{1}H and ^{13}C NMR chemical shifts of **3a** and **3b** have been compared with the experimental data. According to these results, the calculated chemical shifts are in line with the experimental findings. In order to compare the experimental chemical shifts based on the calculations, the correlation graphics have been presented in Fig. 3.

The carbon chemical shifts' correlation values are found to be 0.972 for compound **3b**. As shown in Fig. 3, those compounds have 18 different carbon atoms, which is consistent with the structure based on molecular symmetry. Chemical shifts were reported in parts per million relative to TMS for ^{1}H and ^{13}C NMR spectra. Spectra were obtained at a base frequency of 125.76 MHz for ^{13}C and 500.13 MHz for ^{1}H nuclei. Relative chemical shifts were then estimated by using the corresponding TMS shielding calculated in advance at the same theoretical level as the reference. The experimental values of ^{1}H and ^{13}C isotropic chemical shifts for TMS were 31.78 ppm and 201.576 ppm, respectively.

Electronic structure

The experimental data suggest that the nonphenolic model is less able to suffer photoyellowing, as proposed by Lanzalunga and coworkers [27]. The energy of HOMO and LUMO orbital's showed in Table 6. Fig. 4 presents the spin density isosurface for HOMO and LUMO orbital's of the phenolic and nonphenolic model

Table 5
Experimental and calculated ^{13}C NMR chemical shifts (ppm) of **3a**, **3b** compounds.

Compound	**3a**		3b	
Carbon	DFT	Exp	DFT	Exp
C24	162.20	–	158.68	149.69
C27	161.25	–	158.03	148.01
C1	158.10	–	153.93	147.1
C5	158.02	–	153.42	147.1
C6	148.52	–	153.42	134.1
C3	146.43	–	141.14	132.09
C21	128.64	–	128.84	121.96
C23	127.51	–	127.62	121.1
C25	126.33	–	126.03	114.7
C22	116.37	–	117.79	111.77
C4	115.51	–	115.72	103.8
C2	108.33	–	106.05	103.8
C13	104.47	–	90.97	71.33
C9	89.88	–	88.72	65.58
C15	72.48	–	72.46	61.22
C42	67.79	–	66.54	56.26
C46	67.61	–	63.62	56.26
C32	62.77	–	61.83	55.77
C38	62.41	–	–	–

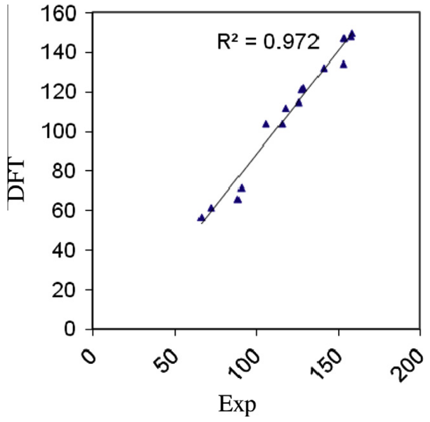

Fig. 3. Plot of the calculated versus the experimental ^{13}C NMR chemical shifts (ppm) of **3b** compound (erythro).

Table 6
Theoretically computed HOMO and LUMO energies (H), ionization potential (H), electron affinity (H), visible absorption maxima (nm), corresponding oscillator strength (eV) for **3a** and **3b** compounds.

Compounds	**3a**		**3b**	
Parameter	HF	DFT	HF	DFT
HOMO energy	−0.30485	−0.21404	−0.30049	−0.21353
LUMO energy	0.06433	−0.01831	0.06397	−0.01316
Ionization potential (IP)	0.30485	0.21404	0.21353	0.21353
Electron affinity (EA)	−0.06433	0.01831	0.01316	0.01316
Visible absorption maxima	215.08	259.76	215.16	256.78
Corresponding oscillator strength	5.7646	4.7731	5.7623	4.8284

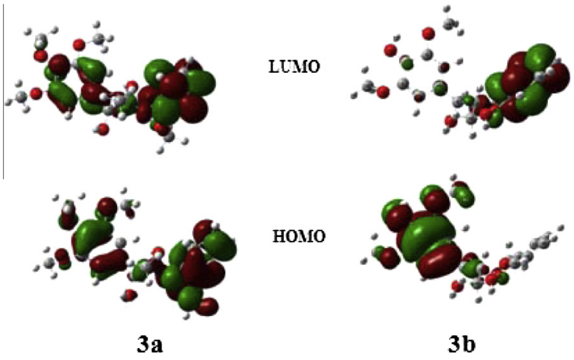

Fig. 4. Spin density isosurface for HOMO and LUMO orbital's of **3a** and **3b** compounds.

(**3a**, **3b** compounds). In HOMO **3a**, the nonzero spin density (clouds over the atoms) occurs on β–O–4 bond and the phenoxy ring and in HOMO **3b** it occurs on carbon and phenyl ring. This is in agreement with the result which is expected for open-shell molecules, where nonzero spin density is an indication of occurrence of unpaired electrons [28,29]. Increase the electron density in the region of -O-4 bond, induces it's strength, imply a higher activation barrier for the cleavage of the β-O-4 bond.

UV–vis spectra

The calculated visible absorption maxima of these compounds in this study are given in Table 6. The electronic spectra of these compounds showed an absorption band in the region 256–259 nm this band was due to electronic transition of the aromatic rings.

Table 7
Theoretically computed energies (H), zero-point vibrational energies (kcal mol^{-1}), rotational constants (GHz), entropies (cal/mol K), and dipole moment (D) for **3a** and **3b** compounds.

Parameters	**3a**	**3b**
Total energy	−1265.02	−1225.73
Zero point energy	257.470	239.400
Rotational constant	0.27504	0.27794
	0.13981	0.15061
	0.11951	0.13026
Entropy		
Total	182.687	176.413
Translational	43.570	43.453
Rotational	35.502	35.332
Vibrational	103.615	100.398
Dipole moment	3.2961	3.9326

Thermodynamic properties

Several calculated thermodynamic parameters of two compounds calculated at B3LYP levels are presented in Table 7.

Conclusions

In previous works LDA was used as base for condensation step that creates an alcohol impurity. Its formation might be due to the reduction of the carbonyl function in aldehyde by a hydride transfer from LDA present in excess. In this study we used hexamethyldisilazane with no α-proton, as base in condensation step. This preclude of this secondary reaction and increase the yield of the condensation step and a diastereoisomeric control can occur using a more sterically crowded enolate that create Z-isomer of propionic acids (2a, 2b). In second step, reduction of these acids (2a, 2b) produces erythro form of products, since hydroboration is known to proceed by syn addition. What higher yields and also in reduction of the amount of a contaminant invariably found in the reaction product was resulted. However, Z- isomer of acid 2a and 2b could be isolated in a yield of 50% and 37%.

No separate deprotection step was required since removal of the tetrahydropyran-2-yl group occurred spontaneously during the reaction (or during the work-up procedure).

The experimental and the theoretical investigation of the title compounds **3a** and **3b** have been performed successfully by using IR and NMR and quantum chemical calculations. This investigation proves that the vibrational frequencies and visible spectra of prepared models can be successfully predicted by HF and B3LYP methods with the used basis sets. According to calculations, the best fittings between calculated and measured vibrational frequencies were achieved by B3LYP theoretical level. With this level, the deviations between calculated and experimental values are quite small for a given type of vibration.

Obtained information about structures, and vibrations are a valuable part of planning chemical experiments, as well as a support for the explanation of obtained experimental results. Thus we can use methods are being used as part of lignin research.

We hope the combination of theoretical and experimental data will be furnished relevant information on the properties and behavior of lignin model compounds and help us to find the photo oxidation mechanism and reactivity of this class of compounds and introduced a new insight about process of photo yellowing.

Acknowledgements

We would like to thank Fars Payame Noor University research council for the financial support (Grant no. 1388/3/0/8/512). Thanks are also due to supports from the Payame Noor University in Isfahan.

References

[1] E. Sjöström, Wood Chemistry. Fundamentals and Application, Academic Press, Orlando, 1993. pp. 293.
[2] D.N.S. Hon, in: D.N.S. Hon, N. Shiraishi (Eds.), Wood and Cellulosic Chemistry, Marcel Decker, New York, 1991, pp. 525–555.
[3] O. Lanzalunga, M. Bietti, J. Photochem. Photobiol. B-Biology 56 (2000) 85–108.
[4] G. Papp, E. Preklet, B. Kosıkova, E. Barta, L. Tolvaj, J. Bohus, S. Szatmari, O. Berkesi, J. Photochem. Photobiol. A-Chem. 163 (2004) 187–192.
[5] A. Sakakibara, in: C.W. Dence, S.Y. Lin (Eds.), Methods in lignin chemistry, Springer-Verlag, Berlin, 1992, pp. 350–368.
[6] F. Lu, J. Ralph, J. Agric. Food Chem. 47 (1999) 1988–1992.
[7] J. Ralph, F. Lu, J. Agric. Food Chem. 46 (1998) 4616–4619.
[8] F. Lu, J. Ralph, J. Wood Chem. Technol. 18 (1988) 219–233.
[9] F. Lu, J. Ralph, J. Agric. Food Chem. 46 (1998) 547–552.
[10] F. Lu, J. Ralph, Phytochemistry 50 (1999) 659–666.
[11] A. Guerra, R. Mendonca, A. Ferraz, F. Lu, J. Ralph, Appl. Environ. Microbiol. 70 (2004) 4073–4078.

[12] F. Lu, J. Ralph, Plant J. 35 (2003) 535–544.
[13] T. Ahvonen, G. Brunow, P. Kristersson, K. Lundquist, Acta Chem. Scand. B 37 (1983) 845–849.
[14] K. Lundquist, S. Remmerth, Acta Chem. Scand. B 29 (1975) 276–278.
[15] S. Li, K. Lundquist, M. Paulsson, Acta Chem. Scand. 49 (1995) 623–624.
[16] K. Lundquist, R. Stomberg, S. Von Ung, Acta Chem. Scand. B 41 (1987) 499–510.
[17] S. Von Unge, K. Lundquist, R. Stomberg, Acta Chem. Scand. B 42 (1988) 469–474.
[18] W. Ibrahim, K. Lundquist, Acta Chem. Scand. 48 (1994) 149–151.
[19] J.Ph. Roblin, H. Duran, V. Banuls, L. Gorrichon, Bioorg. Med. Chem. Lett. 6 (1996) 2355–2358.
[20] V. Namboodiri, R.S. Varma, Tetrahed. Lett. 43 (2002) 1143–1146.
[21] D.C. Young, Computational chemistry, A practical guide for applying techniques to real-world problems, John Wiley & Sons, INC, 2001.
[22] L.M. Proniewicz, C. Paluszkiewicz, A. Weselucha, H. Majcherczyk, A. Baranski, A. Konieczna, J. Mol. Struct. 596 (2001) 163–169.
[23] M. Akerholm, B. Hinterstoisser, L. Salmen, Carbohyd. Res. 339 (2003) 569–578.
[24] G. Socrates, Infrared Characteristic Group Frequencies (2th ed) West Sussex, John Wiley & Sons, UK, 1994.
[25] M. Czaplicka, B. Kaczmarczyk, Talanta. 70 (2006) 940–949.
[26] P.S. Nobel, Physicochemical and Environmental Plant Physiology, third ed., Elsevier Academic press, Burlington, 2005.
[27] C.M. Popescu, P.T. Larsson, N. Olaru, C. Vasile, Carbohyd. Polym. 88 (2012) 530–536.
[28] U. Muller, M. Ratzsch, M. Schwanninger, M. Steiner, H. Zobl, J. Photochem. Photobiol. B-Biology. 69 (2003) 97–105.
[29] W.J. Hehre, J. Yu, P.E. Klunzinger, L. Lou, A Brief Guide to Molecular Mechanics and Quantum Chemical Calculation, Wavefunction Inc., Irvine, USA, 1998.